Molecular Model for the Self-Assembly of the Cyclic Lipodepsipeptide Pseudodesmin A

Jean-Marc Crowet, Davy Sinnaeve, Krisztina Fehér, Yoann Laurin, Magali Deleu, José C. Martins, Laurence Lins

▶ **To cite this version:**

Jean-Marc Crowet, Davy Sinnaeve, Krisztina Fehér, Yoann Laurin, Magali Deleu, et al.. Molecular Model for the Self-Assembly of the Cyclic Lipodepsipeptide Pseudodesmin A. Journal of Physical Chemistry B, 2019, 123 (42), pp.8916-8922. 10.1021/acs.jpcb.9b08035 . hal-02538325

HAL Id: hal-02538325
https://hal.science/hal-02538325

Submitted on 17 Nov 2020

HAL is a multi-disciplinary open access archive for the deposit and dissemination of scientific research documents, whether they are published or not. The documents may come from teaching and research institutions in France or abroad, or from public or private research centers.

L'archive ouverte pluridisciplinaire **HAL**, est destinée au dépôt et à la diffusion de documents scientifiques de niveau recherche, publiés ou non, émanant des établissements d'enseignement et de recherche français ou étrangers, des laboratoires publics ou privés.

Molecular model for the self-assembly of the cyclic lipodepsipeptide Pseudodesmin A

Jean-Marc Crowet[1], Davy Sinnaeve[2], Krisztina Fehér[2], Yoann Laurin[1], Magali Deleu[1], José C. Martins[2], Laurence Lins[1]*

1. Laboratory of Molecular Biophysics at Interfaces, TERRA Research Center, Gembloux Agro-Bio Tech, University of Liège, Passage des déportés 2, B-5030 Gembloux, Belgium
2. NMR and Structure Analysis Unit, Department of Organic and Macromolecular Chemistry, Ghent University, Krijgslaan 281 S4, B-9000 Gent, Belgium
* to whom correspondence should be addressed.

Abstract

Self-assembly of peptides into supramolecular structures represents an active field of research with potential applications ranging from material science to medicine. Their study typically involves the application of a large toolbox of spectroscopic and imaging techniques. However, quite often the structural aspects remain underexposed. Besides, molecular modeling of the self-assembly process is usually difficult to handle since a vast conformational space has to be sampled. Here, we have used an approach that combines short molecular dynamics simulations for peptide dimerization and NMR restraints to build a model of the supramolecular structure from the dimeric units. Experimental NMR data notably provide crucial information about the conformation of the monomeric units, the supramolecular assembly dimensions and the orientation of the individual peptides within the assembly. This *in silico*/*in vitro* mixed approach enables us to define accurate atomistic models of supramolecular structures of the bacterial cyclic lipodepsipeptide pseudodesmin A.

Introduction

Resolving the supramolecular structures adopted by short to medium-sized self-assembling peptide systems is a very challenging task both experimentally and computationally.[1–3] These structures are of increasing interest due to their potential applications in nanotechnology, biotechnology and medicine. Supramolecular assemblies with various morphologies find applications such as drug delivery systems, biosensors, imaging contrasts agents, antimicrobial agents or biomaterials for tissue engineering and biominerialisation.[4–6] Peptides offer a biocompatible, easy to use/synthetically accessible and chemically diverse platform for developing new nanostructures in a controlled fashion. Understanding the forces that drive these building blocks towards self-assembly is of paramount importance for rational design of nanostructures for a specific purpose. Their study by experimental methods typically requires combination of multiple spectroscopic and imaging techniques.[4,7–10]

Higher-order supramolecular structures are hardly amenable to high-resolution approaches such as solution state NMR or X-ray crystallography due to size heterogeneity and/or insolubility.

From a computational point of view, self-assembly is hard to tackle because high level of sampling of the conformational space is required for the convergence of thermodynamic and structural quantities. All-atom molecular dynamic (MD) simulations have limited ability to reach the long time scales required for the sampling of the molecular degree of freedom. This issue is typically addressed by employing advanced sampling techniques or by reducing the number of freedom degrees with coarse grained (CG) representation of molecular entities.[2,11,12]

In this work, we have developed an original approach to circumvent these computational limitations by rationally deducing the supramolecular structures from short MD calculations, guided and validated by NMR experimental data. The system under investigation is the cyclic lipodepsipeptide (CLP) pseudodesmin A,[13] a pseudomonas secondary metabolite of the viscosin group.[14,15] Besides interesting biological activity, it displays remarkable self-assembling properties in non-polar solutions.[16–19] The precise biological role of the self-assembly is yet to be established for this and other CLPs, although it is speculated that it could occur within the cellular membrane bilayer, which is the apparent target of these compounds for antimicrobial activity.[20,21] Pseudodesmin A consists of two moieties: (1) a nonapeptide (L-Leu1-D-Gln2-D-aThr3-D-Val4-D-Leu5-D-Ser6-L-Leu7-D-Ser8-L-Ile9) cyclized via an ester bond between the C-terminal carboxyl and the D-aThr3 side chain hydroxyl and (2) a fatty acid ((R)-3-hydroxydecanoic acid) group attached to the N-terminus of the peptide. The monomer conformation was solved by both NMR and X-ray diffraction, and features a short left-handed α-helix of six amino acids long, followed by a three-residue loop that completes the cyclic structure by covalently stapling the end of the helix to its middle (Fig. 1).[13] The overall molecule is amphipathic, with the hydrophobic and hydrophilic residues grouped along opposite sides of the molecular surface. While no self-assembly was observed in acetonitrile solution, formation of large supramolecular structures has been demonstrated in chloroform.[16] Using of ^{13}C relaxation NMR, it was shown that the assemblies possess axially symmetric shape and grow along one dimension.[17] The estimated dimensions suggested that filaments larger than the diameter of one molecule are formed. Also, the orientation of the monomer units relative to the direction of growth can be established, strongly suggesting that the assembly is mediated via intermolecular contacts between free N-terminal amides as hydrogen bond donors and the C-terminal carbonyls as hydrogen bond acceptors.[17] Intermolecular ROESY (rOe) correlation also confirmed that contacts occurs mainly between these parts of the molecule.[16] However, a detailed atomistic model of the supramolecular assembly remains difficult to established at this stage. For this reason, we decided to combine *in vitro* NMR data with molecular modeling.

Our modeling approach involves three steps: (1) scanning of modes of interaction between two

monomers by multiple, short MD simulations using intramolecular NMR distance restraints, (2) construction of all feasible supramolecular structures based on the computed dimers and (3) selection of the correct filament structure based on the experimental ^{13}C NMR relaxation data obtained in Sinnaeve *et al*. 2012.[17] The complementarity of MD simulations and NMR data is crucial here since each separate technique (*in silico* and *in vitro*) is not sufficient to obtain an accurate atomistic model.

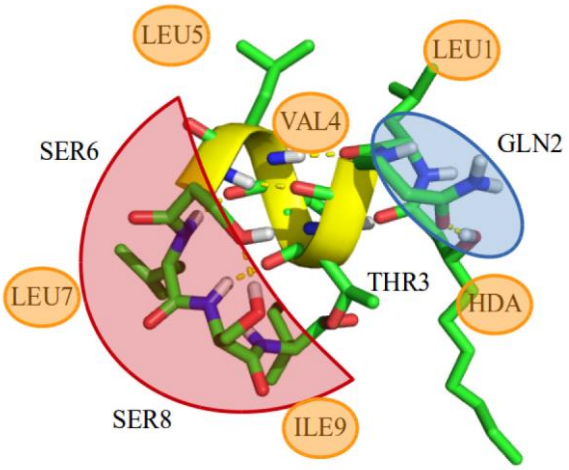

Figure 1: NMR structure of the pseudodesmin A.¹⁶ Carbon hydrogens and backbone carbons of the helix are not represented. The left handed helix cartoon and the hydrogen bonds are in yellow. H bonds donors, H bonds acceptor and hydrophobic amino acids are respectively circled in blue, red and orange.

Methods

Atomistic molecular dynamics

Simulations have been performed with the GROMOS 54a7 force-field.[22] The NMR structure of Pseudodesmin (L-Leu1-D-Gln2-D-aThr3-D-Val4-D-Leu5-D-Ser6-L-Leu7-D-Ser8-L-Ile9 ; Fig. 1) has been used.[13] The D-amino acids and the allo-threonine have been added to force-field by adapting the improper dihedral definition of the alpha and beta carbons respectively. HDA is derived from Threonine and parameters for ester cyclization have been derived from ethyl acetate.[22] The model used to simulate chloroform is the one present natively in the force-field and acetonitrile parameters are coming from ATB repository.[23] rOe distance restraints defined in Sinnaeve *et al*. 2009[16] (Table SI) were used during the molecular dynamics simulations. As the carbon hydrogens are not represented in the Gromos force-fields, 0.1 nm was added to the distance restraints in these cases. All the systems studied were first minimized by steepest descent for 5000 steps. They were then run for a 1 ns simulation with the peptide under position restraints in periodic boundary conditions (PBC) using a 2 fs time step. Production runs were performed for 50 ns. All the systems were solvated with SPC water,[24] chloroform or acetonitrile. The dynamics were carried out in the NPT conditions (298

K and 1 bar). Temperature was maintained by using the v-rescale method[25] with τT = 0.2 ps and an isotropic pressure was maintained by using the Parrinello-Rahman[26] barostat with a compressibility of 4.5 × 10^5 (1/bar) and τP = 1 ps. Electrostatic interactions were treated by using the particle mesh Ewald (PME) method.[27] Van der Waals and electrostatics were treated with a 1.0 nm cut-off. Bond lengths were maintained with the LINCS[28] algorithm. The trajectories were performed and analyzed with the GROMACS 4.5.4 tools as well as with homemade scripts and softwares, and 3D structures were analyzed with both PYMOL[29] and VMD[30] softwares.

Results

Simulation of solvent dependent self-assembly: acetonitrile versus chloroform

In order to reproduce the behavior of the peptides observed experimentally in both acetonitrile (no self-assembly observed) and chloroform (strong self-assembly), we performed short standard MD simulations in these solvents. It has already been established by NMR that the peptide monomer adopts essentially the same intramolecular conformation in both acetonitrile and chloroform.[16] In order to reduce the degrees of motional freedom, intramolecular NMR distance restraints (Table SI) obtained from acetonitrile solution are used here to restrain the peptide structure during the simulations to avoid drifting too far from the experimental conformation. Simulation of four peptides in an acetonitrile solvent box for 250 ns showed that peptides stay mainly monomeric, in agreement with experimental data.[16] Dimers can be formed transiently but represent less than 13.5 % of the simulation time. In contrast, in chloroform, peptides rapidly interact with each other and form multimers during the whole simulation time (Fig. S1). However, due to the many possible modes of intermolecular interaction between the peptides, using a brute-force approach to sample a larger number of peptides in a large solvent box in order to observe the formation of a well-defined supramolecular structure is unlikely to succeed within a reasonable period of time using currently available computational power.

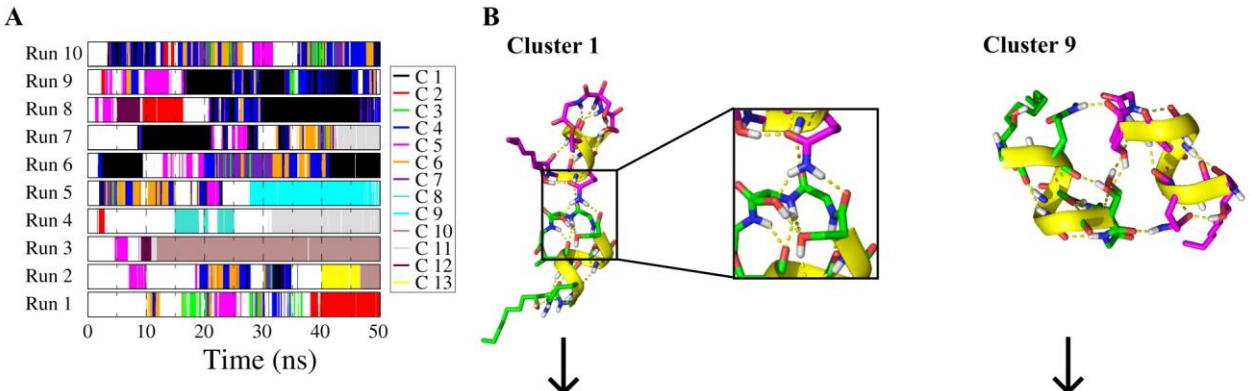

Figure 2: Cluster occurrence and filaments construction. A) Cluster occurrence in each simulation run. **B)** Representation of the dimer from clusters C1 and C9 and their association to build the filaments. Carbon hydrogens and backbone carbons of the helix are not represented. The left-handed helix cartoon and the hydrogen bonds are in yellow. The filaments built from clusters C1 and C9 are drawn with a surface representation. Hydrophobic residues are represented in yellow and pink while hydrophilic residues are represented in green and blue. **C)** Summary table of the pseudodesmin association; pink means no second filament is formed, i.e. molecules do not align (Fig. 2D, right); purple, the second filament forms, but the molecules are not aligned correctly (Fig. 2D, left) and green, the second filament forms in correct way. **D)** Examples of second filaments not correctly formed.

Dimer scan

We chose an alternative approach where we first scan all possible interactions between only two peptides in chloroform. For this, ten independent simulations of 50 ns were carried out (Fig. 2A). Those simulations showed that intermolecular contacts arise mainly through hydrogen bond formation between N-terminal of one peptide and the C-terminal residue of the other, as shown on figure 2B and in agreement with what was already proposed via NMR.[16] Several possible transient intermolecular hydrogen bonds are observed during the simulation time, and most often several hydrogen bonds are formed simultaneously (Table SII). Hydrogen bonding patterns that are associated to specific dimeric organizations can be identified and can be used as a criterion to define dimer structures (Fig. S2). Thirteen clusters were hence classified, each representing at least 0.5% of the total simulation time. Their hydrogen bonds are listed on Table I and SII and represented on figures 2A and S2. Three main types of clusters are observed based on the relative orientation of the peptides: (1) both peptides stacked linearly upon each other via their N- and C-terminal sides (Fig. 2B, left); (2) both peptides aggregated side-by-side in an antiparallel fashion (Fig. 2B, right); (3) both

peptides oriented in a perpendicular arrangement for one cluster (C13) (Table I and Fig. S3). The clusters showing the longer time duration are the anti-parallel dimers C9 to C11 and the two linear clusters C1 and C2 (Table I).

Table I: H-bonds defining each cluster. NH_2 Z corresponds to the H which is on the O side of the planar amide bond (Fig. 2B). OT corresponds to the oxygen of the alkoxy group.

Cluster	Relative orientation	Hydrogen bonds criterion	Cluster	Relative orientation	Hydrogen bonds criterion
Cluster 1	linear	GLN2 NH – LEU7 CO GLN2 NH_2 *E* – SER6 CO	**Cluster 8**	linear	HDA OH – VAL4 CO LEU1 NH – LEU5 CO GLN2 NH – SER6 CO GLN2 NH_2 *E* – LEU7 CO
Cluster 2	linear	LEU1 NH – LEU7 CO GLN2 NH_2 *Z* – SER8 CO			
Cluster 3	linear	LEU1 NH – SER6 CO GLN2 NH_2 *Z* – LEU5 CO	**Cluster 9**	anti-parallel	GLN2 NH_2 *E* – SER6 CO SER6 CO – GLN2 NH_2 *E*
Cluster 4	linear	LEU1 NH – LEU7 CO GLN2 NH_2 *Z* – SER6 CO	**Cluster 10**	anti-parallel	GLN2 NH_2 *E* – SER8 OH SER8 OH – GLN2 NH_2 *E*
Cluster 5	linear	LEU1 NH – SER8 CO GLN2 NH_2 *Z* – LEU7 CO	**Cluster 11**	anti-parallel	GLN2 NH_2 *E* – SER8 CO SER6 CO – GLN2 NH_2 *E*
Cluster 6	linear	HDA OH – SER6 CO LEU1 NH – LEU7 CO GLN2 NH_2 *Z* – LEU5 CO	**Cluster 12**	anti-parallel	GLN2 NH_2 *E* – LEU5 CO SER8 CO – GLN2 NH_2 *E*
Cluster 7	linear	HDA OH – LEU5 CO LEU1 NH – SER6 CO GLN2 NH_2 *Z* – VAL4 CO	**Cluster 13**	perpendicular	GLN2 NH – SER8 CO GLN2 NH_2 *E* – SER8 OH GLN2 NH_2 *Z* – THR3 OT

Construction of one filament supramolecular structures

In the linear dimers, the peptides interact via the hydrogen bond donor side of one molecule and the acceptor side of the other one (cluster C1 of the Fig. 2B) and can then lead to the oligomerization of the peptides. Filamentous oligomers have been built by iterative translations and rotations (Fig. 2B). First, from one member of the dimers, translations and rotations necessary to find the coordinates of the second member of the dimer are computed (Fig. 2B, below). From this transformation matrix, filamentous oligomers that retain the dimer structure and intermolecular contacts are built. For example, the filament formed from cluster C1 shows a helically twisted structure with 5 peptides per turn and all the hydrophilic residues facing inwards (Fig. 2). Different results are obtained from the various other linear clusters, as summarized in figure S4.

Validation of filamentous structures based on NMR data

Experimental NMR results provided the orientation of the monomer within the supramolecular structure relative to the direction of growth.[17] This information can be directly confronted with the filaments obtained by molecular modeling. This orientation is reflected in the collection of angles between various Cα-Hα bonds of each amino acid and the direction of growth (long axis) of the

supramolecular structure, as this is what was obtained from the NMR ^{13}C relaxation approach.[17] The clusters giving filament models displaying the best correlation with experimental data are clusters C1, C2, C4 and C5 with average differences over 10 angles of 13.5°, 10°, 10° and 13.6° while the cluster displaying the greatest differences is cluster C7 with an average difference of 20.6° (Fig. 3, Table SIII).

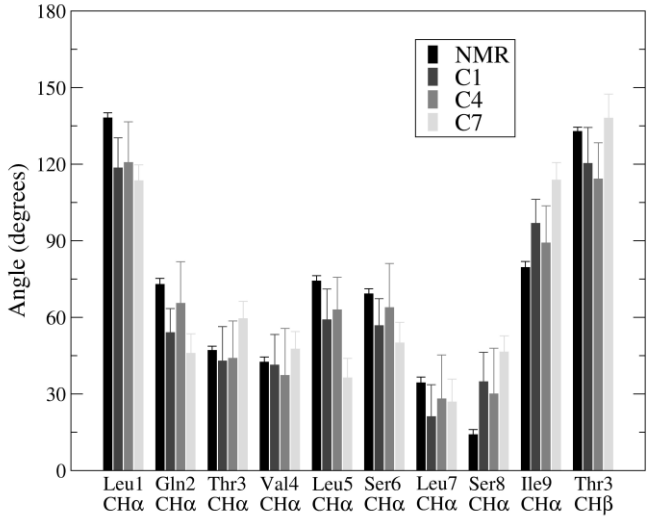

Figure 3: Correlation between NMR ^{13}C relaxation data and C1, C4 or C7 structures about the angles between CαH and the long axis of the filament for each residue.

Construction of the two stranded filament structures

The segregation of hydrophobic and hydrophilic residues along some filaments (see for example Fig. 2B, left or Fig. S4, cluster C1 or C4) strongly suggests that pseudodesmin A can form intertwisted filaments by association of the hydrophilic residues. Cluster C1 and C4, with 5 and 7 peptides per turn are very good candidates, while the other filaments have 4 or less peptides per turn, with some hydrophilic residues facing outside and should then be less prone to self-assemble. To build the second filament, the antiparallel dimers have been used as template. The translations and rotations necessary to go from one member of the antiparallel dimer to the other are computed and applied to each peptide of the linear filament. The 8 linear filament models and the 4 antiparallel dimers have been used to build double stranded filaments (Fig. S5). When we look at Table I, one can notice that the hydrogen bonds defining linear and antiparallel dimers both involves the side chain of GLN2. It supposes that the conformation of the side chain of GLN2 is different in the two structures used to build double stranded filaments, as clearly illustrated on figure 2B for C1 and C9. So, to build double filament, the conformation of the side chain of GLN2 from the linear dimer has been kept, while the hydrogen bonds formed between hydroxyl group of SER6 and SER8 of each peptide in the antiparallel configuration (Fig. 2B and SIV) have been conserved. When looking at the anti-parallel

clusters, C9 is the one where the hydrophilic faces are matching at best (Fig. S3) and from the 32 possible double stranded filaments built, two combinations (C1+9) and (C4+9) give a second filament which is structurally identical to the one-strand filament and are thus the best candidates. It is worth noting that from two unrelated dimer configurations (linear and anti-parallel), a structure with two structurally identical filaments can be built, strongly suggesting self-consistency of the approach. Besides, we can notice on figure 2A that C1 and C4 are frequently observed concomitantly during the simulations while C1 appears to be more stable over time. Since C9 is present during almost all the simulation time (Fig. 2A), we can assume that the two double filament structures could exist as "metastable" conformations that can switch from one to the other.

To further validate our filament models, intermolecular ROESY correlations measured by NMR on the aggregates[16] highlighting molecular contacts can be compared to those observed between the peptides inside the model filament structures. From Table II listing the interatomic distances computed on the cluster models, it is obvious that almost all contacts can be explained by the formation of one or the other linear filaments, clusters C1 and C2 presenting notably seven interatomic distances lower than 5Å. Regarding the other filament candidate made from clusters C4 and C9, it can explain five of the interatomic distances and notably the contact between LEU1 and LEU7 which is not observed in the C1+9 double filaments. We can also notice that the anti-parallel configurations reflects the proximity between the side chain of GLN2 and the backbone of SER8. While, its proximity with ILE9 residue is less obvious. The latter being in the middle of the hydrophobic face of the peptide, no cluster presents interatomic distances smaller than 5Å, except in cluster C13, which is however in a perpendicular configuration. Finally, we compared the diameter measured on the two stranded filament models C1+9 and C4+9 (is 2.1 and 2.3 nm respectively) to the diameter of the aggregate measured by NMR (2.5 nm),[19] showing a very good agreement. On the other hand, the length of aggregates measured by NMR is 6.4 nm,[17] corresponding to structures with an average of 5 and 4 peptides per filament in the C1+9 (6.4 nm) and C4+9 (6.2 nm) models, respectively. Overall, there is a very good agreement between the proposed models for double stranded filaments and the NMR data, strongly supporting our modeling approach.

Table II: List of the atomic contacts determined experimentally by NMR and the interatomic distance computed in each model dimer cluster

	C1	**C2**	**C3**	**C4**	**C5**	**C6**	**C7**	**C8**	**C9**	**C10**	**C11**	**C12**	**C13**
HDA HA – SER8 HA	**4.6**	**5.0**	10.4	**3.6**	**4.5**	**4.2**	8.3	10.3	9.8	11.0	6.9	9.8	8.4

HDA OH – SER8 HA	**3.2**	**3.8**	9.0	**4.8**	**3.3**	5.7	9.0	7.7	7.7	7.9	**3.9**	7.5	6.9
LEU1 HN – LEU7 HA	6.4	**4.0**	5.4	**3.3**	7.9	**2.9**	**3.2**	**5.0**	10.5	13.1	9.6	10.8	9.6
LEU1 HN – SER8 HA	**2.7**	**3.1**	7.8	**3.8**	**3.7**	**4.4**	6.6	8.7	10.4	9.4	5.9	7.3	5.9
LEU1 HN – ILE9 HB	6.9	8.0	12.2	8.7	5.9	9.6	10.9	11.7	16.3	9.8	9.9	11.3	**4.6**
GLN2 HN – LEU7 HA	**4.1**	7.0	**3.8**	**3.9**	7.7	**4.0**	**4.2**	**3.3**	8.1	11.0	7.9	9.2	8.8
GLN2 HN – SER8 HA	**3.1**	**4.0**	7.3	6.3	**4.5**	7.2	8.5	6.7	8.6	7.9	5.7	5.5	**4.6**
GLN2 HN – ILE9 HB	8.7	8.5	11.5	11.0	7.0	11.8	11.6	11.1	14.1	9.5	8.3	8.2	6.6
GLN2 NH_2 *E* – SER8 HA	**3.9**	**4.9**	8.5	8.2	**4.4**	9.4	9.6	**3.6**	**4.9**	**4.4**	**4.3**	**4.0**	**4.5**
GLN2 NH_2 *Z* – SER8 HA	**2.8**	**3.5**	8.4	7.1	**2.8**	7.9	8.3	**4.5**	**4.4**	**4.9**	**3.6**	**4.8**	5.2

Distance lower than 5Å are in bold.

Discussion

The description of peptide self-assembly in order to reach molecular models at atomistic level remains a non trivial and non-obvious task both experimentally and computationally but is of paramount importance for the rational design of nanostructures with specific purposes. To study the peptide self-assembly by experimental methods, it typically requires combination of multiple spectroscopic (NMR, FTIR, CD spectroscopy,...) and imaging techniques (TEM, AFM, …) because supramolecular structures are less amenable to high-resolution approaches such as solution state NMR or X-ray crystallography.[31] The peptide under investigation in this study, Pseudodesmin A, has been the object of an in depth experimental characterization through various NMR and X-ray diffraction techniques.[13,16,17] Experimental NMR data obtained in chloroform notably provide significant information about the conformation of the monomeric units, the supramolecular assembly dimensions and the orientation and intermolecular contacts of the individual peptides within the assembly.[15] However, while very informative, these data were not sufficient to reach an atomistic representation of the aggregates.

Here, we have used an original approach that combines short molecular dynamics simulations of the dimers and NMR restraints to build a model of the supramolecular structure from the dimeric units. The first step of the approach is to calculate dimers of the peptide based on its restrained NMR monomer structure by multiple short MD simulations. Sampling dimer formation and hydrogen bond patterning led us to classify the dimers into 13 clusters in which intermolecular contacts arise mainly through hydrogen bond formation between N-terminal part of one peptide and the C-terminal residue of the other, in agreement with NMR data.[15] The dimers can either be linear or anti-parallel. More precisely, we found that the interactions and peptide configurations observed for the linear cluster C1 are very favorable to filament formation, according to NMR data. Moreover, this filament presents a

partition of its hydrophobic and hydrophilic residue that allows the formation of complementary and identical filaments, when combined to the anti-parallel cluster C9. In addition, these two clusters are the ones that are the more populated during molecular dynamics simulations. Another potential structure is made of C9 and C4 clusters, which presents these same properties. Both oligomeric structures converge, strongly supporting our methodology. The oligomeric structure further appears to fit all the available experimental information (intermolecular contacts, orientation, shape and size) and provides now a working model of the Pseudodesmin self-assembly.

It should be noted that simulating self-assembly processes by MD is not an obvious task and all-atom molecular dynamics (AT-MD) simulations have limited ability to reach the long time scales required for the sampling of the molecular degrees of freedom associated with the self-assembly.[32,33] The formation of small oligomers, the earliest stages of the self-assembly, can be performed by AT-MD, usually with advanced sampling techniques such as replica exchange molecular dynamics (REMD).[32,34–38] Multiscale approaches using REMD and implicit water forcefield such as OPEP coupled to all atom MD simulations notably allowed to simulate the self organization of Sup35 amyloid peptides without pre-formed seeds.[12] In the same way, activation-relaxation technique (ART) simulations allowing to sample the energy landscape, were coupled to coarse grained energy models and AT MD simulations to study the early steps of amyloid peptide aggregation.[39] These advanced techniques are required to sample the conformational space of monomers to find the ones involved in the oligomers. In our study, the high stability of the peptide conformation as a monomer and in aggregates allow us, by using NMR restraints on monomers, to directly sample the dimerization processes by using short AT-MD simulations. MD also allows to simulate the dimerization in the same environment as experimentally (chloroform or acetonitrile). For the formation of larger oligomers, the process eventually leading to nanostructures like fibrils or nanotubes, simulations using a coarse grained (CG) representation reducing the number of freedom degrees, have been successfully applied in simulating the formation of nanostructures,[2,40,41] like fibrils of Aβ peptide,[35] cylindrical micelle fiber by peptide amphiphiles.[42] However, CG-MD simulations are not always sufficiently accurate to study self-assembly.[43] In our study, CG representation like MARTINI cannot be used due to the limitation of this method in reproducing hydrogen bond interactions.[43] Indeed, this peptide has a hydrogen bond donor side and an acceptor side that could not be distinguished in a CG representation. To address self assembly in this context, the well defined dimer structures identified during the dimerization simulation enabled the exploration of larger oligomers structures and allowed the identification of accurate model filament candidates. To study the later stage of self-assembly, model aggregates are usually preformed prior to AT-MD simulations, such as preformed amyloid fibrils built by stacking beta strands[44–47] or peptides assembled into cylindrical nanofibers.[48,49] In contrast to Pseudodesmin A, these peptides do not have a well-defined

conformation and present a wide range of interactions inside the aggregates.[9,10,50] A way to solution this problem is to validate these interactions against experimental information like intermolecular contacts identified by NMR.[9,51,52] In our study, experimental observations also help to build and validate the aggregate structure obtained by simulations. The complementarity of MD simulations and NMR data is crucial here since each separate technique (*in silico* and *in vitro*) was not sufficient to obtain an accurate atomistic model.

In conclusion, we have used a fast MD and modelling approach to obtain supramolecular structure at the atomistic level, since sampling of the dimers are made with short simulation times. Model filaments can be build from the computed dimer structures, by using NMR data to guide and validate atomistic models step by step. Our original *in silico*/*in vitro* approach has allowed to solve a harsh structural problem, i.e. peptide self-assembly for a cyclic aggregating peptide, pseudodesmin A. This stumbling block would not have been solved by CG-MD methods or AT-MD bruteforce only. The proposed strategy could hence be applied to other aggregating peptides having a conformational stability as monomer or dimer and could be used for rational design of nanostructures for specific purposes.

Supporting Information

Acknowledgments

LL and MD thank the FRS-FNRS for financial support. This work is supported by the FRS-FNRS (BRIDGING CDR J.0114.18 and RHAMEMB CDR J.0086.18, PDR T.0063.19). Partial computational resources have been provided by the Consortium des Équipements de Calcul Intensif (CÉCI), funded by the Fonds de la Recherche Scientifique de Belgique (F.R.S.-FNRS) under Grant No. 2.5020.11.

References

(1) Colombo, G.; Soto, P.; Gazit, E. Peptide Self-Assembly at the Nanoscale: A Challenging Target for Computational and Experimental Biotechnology. *Trends Biotechnol.* **2007**, *25* (5), 211–218.

(2) Frederix, P. W. J. M.; Patmanidis, I.; Marrink, S. J. Molecular Simulations of Self-Assembling Bio-Inspired Supramolecular Systems and Their Connection to Experiments. *Chem. Soc. Rev.* **2018**, *47* (10), 3470–3489.

(3) Tuttle, T. Computational Approaches to Understanding the Self-Assembly of Peptide-Based Nanostructures. *Isr. J. Chem.* **2015**, *55* (6–7), 724–734.

(4) Mandal, D.; Nasrolahi Shirazi, A.; Parang, K. Self-Assembly of Peptides to Nanostructures. *Org. Biomol. Chem.* **2014**, *12* (22), 3544–3561.

(5) Qiu, F.; Chen, Y.; Tang, C.; Zhao, X. Amphiphilic Peptides as Novel Nanomaterials: Design, Self-Assembly and Application. *Int. J. Nanomedicine* **2018**, *Volume 13*, 5003–5022.

(6) Eskandari, S.; Guerin, T.; Toth, I.; Stephenson, R. J. Recent Advances in Self-Assembled Peptides: Implications for Targeted Drug Delivery and Vaccine Engineering. *Adv. Drug Deliv. Rev.* **2017**, *110–111*, 169–187.

(7) Nieuwland, M.; Ruizendaal, L.; Brinkmann, A.; Kroon-Batenburg, L.; van Hest, J. C. M.; Löwik, D. W. P. M. A Structural Study of the Self-Assembly of a Palmitoyl Peptide Amphiphile. *Faraday Discuss.* **2013**, *166* (0), 361.

(8) Hollamby, M. J.; Karny, M.; Bomans, P. H. H.; Sommerdjik, N. A. J. M.; Saeki, A.; Seki, S.; Minamikawa, H.; Grillo, I.; Pauw, B. R.; Brown, P.; et al. Directed Assembly of Optoelectronically Active Alkyl–π-Conjugated Molecules by Adding n-Alkanes or π-Conjugated Species. *Nat. Chem.* **2014**, *6* (8), 690–696.

(9) Rad-Malekshahi, M.; Visscher, K. M.; Rodrigues, J. P. G. L. M.; de Vries, R.; Hennink, W. E.; Baldus, M.; Bonvin, A. M. J. J.; Mastrobattista, E.; Weingarth, M. The Supramolecular Organization of a Peptide-Based Nanocarrier at High Molecular Detail. *J. Am. Chem. Soc.* **2015**, *137* (24), 7775–7784.

(10) Yu, Z.; Erbas, A.; Tantakitti, F.; Palmer, L. C.; Jackman, J. A.; Olvera de la Cruz, M.; Cho, N.-J.; Stupp, S. I. Co-Assembly of Peptide Amphiphiles and Lipids into Supramolecular Nanostructures Driven by Anion−π Interactions. *J. Am. Chem. Soc.* **2017**, *139* (23), 7823–7830.

(11) Yuan, C.; Li, S.; Zou, Q.; Ren, Y.; Yan, X. Multiscale Simulations for Understanding the Evolution and Mechanism of Hierarchical Peptide Self-Assembly. *Phys. Chem. Chem. Phys.* **2017**, *19* (35), 23614–23631.

(12) Nasica-Labouze, J.; Meli, M.; Derreumaux, P.; Colombo, G.; Mousseau, N. A Multiscale Approach to Characterize the Early Aggregation Steps of the Amyloid-Forming Peptide GNNQQNY from the Yeast Prion Sup-35. *PLoS Comput. Biol.* **2011**, *7* (5), e1002051.

(13) Sinnaeve, D.; Michaux, C.; Van hemel, J.; Vandenkerckhove, J.; Peys, E.; Borremans, F. a. M.; Sas, B.; Wouters, J.; Martins, J. C. Structure and X-Ray Conformation of Pseudodesmins A and B, Two New Cyclic Lipodepsipeptides from Pseudomonas Bacteria. *Tetrahedron* **2009**, *65* (21), 4173–4181.

(14) Raaijmakers, J. M.; de Bruijn, I.; de Kock, M. J. D. Cyclic Lipopeptide Production by Plant-Associated Pseudomonas Spp.: Diversity, Activity, Biosynthesis, and Regulation. *Mol. Plant. Microbe. Interact.* **2006**, *19* (7), 699–710.

(15) Gross, H.; Loper, J. E. Genomics of Secondary Metabolite Production by Pseudomonas Spp. *Nat. Prod. Rep.* **2009**, *26* (11), 1408.

(16) Sinnaeve, D.; Hendrickx, P. M. S.; Van Hemel, J.; Peys, E.; Kieffer, B.; Martins, J. C. The Solution Structure and Self-Association Properties of the Cyclic Lipodepsipeptide Pseudodesmin A Support Its Pore-Forming Potential. *Chem. Eur. J.* **2009**, *15* (46), 12653–12662.

(17) Sinnaeve, D.; Delsuc, M.-A.; Martins, J. C.; Kieffer, B. Insight into Peptide Self-Assembly from Anisotropic Rotational Diffusion Derived from 13C NMR Relaxation. *Chem. Sci.* **2012**, *3* (4), 1284.

(18) De Vleeschouwer, M.; Sinnaeve, D.; Van den Begin, J.; Coenye, T.; Martins, J. C.; Madder, A. Rapid Total Synthesis of Cyclic Lipodepsipeptides as a Premise to Investigate Their Self-Assembly and Biological Activity. *Chem. - A Eur. J.* **2014**, *20* (25), 7766–7775.

(19) Geudens, N.; De Vleeschouwer, M.; Fehér, K.; Rokni-Zadeh, H.; Ghequire, M. G. K.; Madder, A.; De Mot, R.; Martins, J. C.; Sinnaeve, D. Impact of a Stereocentre Inversion in Cyclic Lipodepsipeptides from the Viscosin Group: A Comparative Study of the Viscosinamide and Pseudodesmin Conformation and Self-Assembly. *ChemBioChem* **2014**, *15* (18), 2736–2746.

(20) Geudens, N.; Nasir, M. N.; Crowet, J.-M.; Raaijmakers, J. M.; Fehér, K.; Coenye, T.; Martins, J. C.; Lins, L.; Sinnaeve, D.; Deleu, M. Membrane Interactions of Natural Cyclic Lipodepsipeptides of the Viscosin Group. *Biochim. Biophys. Acta - Biomembr.* **2017**, *1859* (3), 331–339.

(21) Khavani, M.; Izadyar, M.; Housaindokht, M. R. Theoretical Design of the Cyclic Lipopeptide Nanotube as a Molecular Channel in the Lipid Bilayer, Molecular Dynamics and Quantum Mechanics Approach. *Phys. Chem. Chem. Phys.* **2015**, *17* (38), 25536–25549.

(22) Schmid, N.; Eichenberger, A. P.; Choutko, A.; Riniker, S.; Winger, M.; Mark, A. E.; van Gunsteren, W. F. Definition and Testing of the GROMOS Force-Field Versions 54A7 and 54B7. *Eur. Biophys. J.* **2011**, *40* (7), 843–856.

(23) Malde, A. K.; Zuo, L.; Breeze, M.; Stroet, M.; Poger, D.; Nair, P. C.; Oostenbrink, C.; Mark, A. E. An Automated Force Field Topology Builder (ATB) and Repository: Version 1.0. *J. Chem. Theory Comput.* **2011**, *7* (12), 4026–4037.

(24) Hermans, J.; Berendsen, H. J. C.; Van Gunsteren, W. F.; Postma, J. P. M. A Consistent Empirical Potential for Water-Protein Interactions. *Biopolymers* **1984**, *23* (8), 1513–1518.

(25) Bussi, G.; Donadio, D.; Parrinello, M. Canonical Sampling through Velocity Rescaling. *J. Chem. Phys.* **2007**, *126* (1), 014101.

(26) Parrinello, M. Polymorphic Transitions in Single Crystals: A New Molecular Dynamics Method. *J. Appl. Phys.* **1981**, *52* (12), 7182.

(27) Essmann, U.; Perera, L.; Berkowitz, M. L.; Darden, T.; Lee, H.; Pedersen, L. G. A Smooth Particle Mesh Ewald Method. *J. Chem. Phys.* **1995**, *103* (19), 8577.

(28) Hess, B.; Bekker, H.; Berendsen, H. J. C.; Fraaije, J. G. E. M. LINCS: A Linear Constraint Solver for Molecular Simulations. *J. Comput. Chem.* **1997**, *18* (12), 1463–1472.

(29) Schrödinger, L. L. C. The PyMOL Molecular Graphics System, Version 1.3. *Methods Enzymol.* **2010**, *266*, 540–553.

(30) Humphrey, W.; Dalke, A.; Schulten, K. VMD: Visual Molecular Dynamics. *J. Mol. Graph.* **1996**, *14* (1), 33–38, 27–28.

(31) Ekiz, M. S.; Cinar, G.; Khalily, M. A.; Guler, M. O. Self-Assembled Peptide Nanostructures for Functional Materials. *Nanotechnology* **2016**, *27* (40), 402002.

(32) Morriss-Andrews, A.; Shea, J.-E. Simulations of Protein Aggregation: Insights from Atomistic and Coarse-Grained Models. *J. Phys. Chem. Lett.* **2014**, *5* (11), 1899–1908.

(33) Manandhar, A.; Kang, M.; Chakraborty, K.; Tang, P. K.; Loverde, S. M. Molecular Simulations of Peptide Amphiphiles. *Org. Biomol. Chem.* **2017**, *15* (38), 7993–8005.

(34) Moore, S.; Sonar, K.; Bharadwaj, P.; Deplazes, E.; Mancera, R. Characterisation of the Structure and Oligomerisation of Islet Amyloid Polypeptides (IAPP): A Review of Molecular Dynamics Simulation Studies. *Molecules* **2018**, *23* (9), 2142.

(35) Shea, J.-E.; Urbanc, B. Insights into Aβ Aggregation: A Molecular Dynamics Perspective. *Curr. Top. Med. Chem.* **2012**, *12* (22), 2596–2610.

(36) Redler, R. L.; Shirvanyants, D.; Dagliyan, O.; Ding, F.; Kim, D. N.; Kota, P.; Proctor, E. a; Ramachandran, S.; Tandon, A.; Dokholyan, N. V. Computational Approaches to Understanding Protein Aggregation in Neurodegeneration. *J. Mol. Cell Biol.* **2014**, *6* (2), 104–115.

(37) Ning, L.; Guo, J.; Bai, Q.; Jin, N.; Liu, H.; Yao, X. Structural Diversity and Initial Oligomerization of PrP106-126 Studied by Replica-Exchange and Conventional Molecular Dynamics Simulations. *PLoS One* **2014**, *9* (2), e87266.

(38) Gee, J.; Shell, M. S. Two-Dimensional Replica Exchange Approach for Peptide-Peptide Interactions. *J. Chem. Phys.* **2011**, *134* (6), 064112.

(39) Mousseau, N.; Derreumaux, P. Exploring the Early Steps of Amyloid Peptide Aggregation by Computers. *Acc. Chem. Res.* **2005**, *38* (11), 885–891.

(40) Liu, D.; Liu, F.; Zhou, W.; Chen, F.; Wei, J. Molecular Dynamics Simulation of Self-Assembly and Viscosity Behavior of PAM and CTAC in Salt-Added Solutions. *J. Mol. Liq.* **2018**, *268*, 131–139.

(41) Sasselli, I. R.; Moreira, I. P.; Ulijn, R. V.; Tuttle, T. Molecular Dynamics Simulations Reveal Disruptive Self-Assembly in Dynamic Peptide Libraries. *Org. Biomol. Chem.* **2017**, *15* (31), 6541–6547.

(42) Lee, O.-S.; Cho, V.; Schatz, G. C. Modeling the Self-Assembly of Peptide Amphiphiles into Fibers Using Coarse-Grained Molecular Dynamics. *Nano Lett.* **2012**, *12* (9), 4907–4913.

(43) Marrink, S. J.; Tieleman, D. P. Perspective on the Martini Model. *Chem. Soc. Rev.* **2013**, *42* (16), 6801–6822.

(44) Gautieri, A.; Milani, A.; Pizzi, A.; Rigoldi, F.; Redaelli, A.; Metrangolo, P. Molecular Dynamics Investigation of Halogenated Amyloidogenic Peptides. *J. Mol. Model.* **2019**, *25* (5), 124.

(45) Rigoldi, F.; Metrangolo, P.; Redaelli, A.; Gautieri, A. Nanostructure and Stability of Calcitonin Amyloids. *J. Biol. Chem.* **2017**, *292* (18), 7348–7357.

(46) Bertran, O.; Curcó, D.; Zanuy, D.; Alemán, C. Atomistic Organization and Characterization of Tube-like Assemblies Comprising Peptide–Polymer Conjugates: Computer Simulation Studies. *Faraday Discuss.* **2013**, *166*, 59.

(47) Vijayaraj, R.; Van Damme, S.; Bultinck, P.; Subramanian, V. Structure and Stability of Cyclic Peptide Based Nanotubes: A Molecular Dynamics Study of the Influence of Amino Acid Composition. *Phys. Chem. Chem. Phys.* **2012**, *14* (43), 15135.

(48) Lee, O.-S.; Stupp, S. I.; Schatz, G. C. Atomistic Molecular Dynamics Simulations of Peptide Amphiphile Self-Assembly into Cylindrical Nanofibers. *J. Am. Chem. Soc.* **2011**, *133* (10), 3677–3683.

(49) Kang, M.; Chakraborty, K.; Loverde, S. M. Molecular Dynamics Simulations of Supramolecular Anticancer Nanotubes. *J. Chem. Inf. Model.* **2018**, *58* (6), 1164–1168.

(50) Lee, O.-S.; Stupp, S. I.; Schatz, G. C. Atomistic Molecular Dynamics Simulations of Peptide Amphiphile Self-Assembly into Cylindrical Nanofibers. *J. Am. Chem. Soc.* **2011**, *133* (10), 3677–3683.

(51) Cormier, A. R.; Pang, X.; Zimmerman, M. I.; Zhou, H.-X.; Paravastu, A. K. Molecular Structure of RADA16-I Designer Self-Assembling Peptide Nanofibers. *ACS Nano* **2013**, *7* (9), 7562–7572.

(52) Nagy-Smith, K.; Moore, E.; Schneider, J.; Tycko, R. Molecular Structure of Monomorphic Peptide Fibrils within a Kinetically Trapped Hydrogel Network. *Proc. Natl. Acad. Sci.* **2015**, *112* (32), 9816–9821.